Available online at www.sciencedirect.com
ScienceDirect
Journal of Catalysis 254 (2008) 226–237
JOURNAL OF CATALYSIS
www.elsevier.com/locate/jcat

Mechanistic analogies and differences between gold- and palladium-supported Schiff base complexes as hydrogenation catalysts: A combined kinetic and DFT study

Aleix Comas-Vives [a], Camino González-Arellano [b,c], Mercè Boronat [d], Avelino Corma [d,*], Marta Iglesias [c], Félix Sánchez [b], Gregori Ujaque [a,*]

[a] *Unitat de Química Física, Departament de Química, Edifici C.n., Universitat Autònoma de Barcelona, 08193 Bellaterra, Catalonia, Spain*
[b] *Instituto de Química Orgánica General, CSIC, C/Juan de la Cierva 3, 28006 Madrid, Spain*
[c] *Instituto de Ciencia de Materiales de Madrid, CSIC, C/Sor Juana Inés de la Cruz 3, Cantoblanco, 28049 Madrid, Spain*
[d] *Instituto de Tecnología Química, UPV-CSIC, Universidad Politécnica de Valencia, Av. de los Naranjos, s/n, 46022 Valencia, Spain*

Received 17 July 2007; revised 13 November 2007; accepted 24 December 2007

Abstract

The mechanism of olefin hydrogenation catalyzed by Pd^{II} and Au^{III} Schiff base complexes, both with an analog d^8 electronic structure, is analyzed by means of kinetic and computational methods. The computational study is able to explain the differences experimentally observed in relation to the influence of the solvent (polarity and proton donor ability) and of the hydrogen pressure on the Au^{III}- and Pd^{II}-catalyzed reaction mechanisms. These considerations can guide the proper selection of solid supports for heterogenization of catalysts to significantly increase their activity.

Keywords: Density functional calculations; Mechanism; Catalysis; Hydrogenation

1. Introduction

Whereas platinum, palladium, and rhodium have been used for decades as catalysts in various homogeneous and heterogeneous reactions [1–6], gold was long believed to be chemically inert. Only in recent years have gold complexes and gold supported on different carriers attracted much interest as catalysts [7–9]. Small-crystal size gold supported on inorganic oxides or carbon (particle size $\leqslant$5 nm) are highly active and selective for such reactions as CO oxidation at low temperature [10–13], water–gas shift [14], alcohol oxidation [15,16], carbon–carbon bond formation reactions [17], and chemoselective reduction of substituted nitroarenes [18]. Homogeneous gold complexes have been applied in cross-coupling and homocoupling reactions, as well as in hydrogenation of alkenes and imines [19]. Because Au^{III} and Pd^{II} have the same d^8 electronic structure, similar behavior could be expected for Au^{III} and Pd^{II} complexes, at least for some reactions. Consequently, to gain insight into the similarities and differences in reactivity between species that have similar electronic compositions at the outer shell but other differences that can affect their reactivity, we compared the mechanism of olefin hydrogenation catalyzed by two well-defined single-site molecular catalysts formed by Au^{III} and Pd^{II} organic complexes. We carried out kinetic experiments to evaluate the catalytic performance of different heterogenized Schiff base complexes of Au^{III} and Pd^{II} for the hydrogenation of diethyl ethylidensuccinates, and studied the effect of reaction variables on the kinetics of the reaction. The experimental results suggest that a slightly different mechanism should operate in the 2 catalysts. Consequently, we carried out a detailed computational study of the mechanism of olefin hydrogenation catalyzed by a Pd^{II} complex using density functional theory methods and compared the results with those obtained previously for Au^{III} catalysis [20]. The computational

* Corresponding authors. Faxes: +34 96 3877809, +34 93 5812920.
E-mail addresses: acorma@itq.upv.es (A. Corma), Gregori.Ujaque@uab.es (G. Ujaque).

0021-9517/$ – see front matter
doi:10.1016/j.jcat.2007.12.015

study was able to explain the differences observed experimentally between the 2 catalytic systems.

2. Experimental

The synthesis and characterization of homogeneous and heterogenized ligands and metal-complexes is fully described in the Supplementary material [21,22].

2.1. Catalytic experiments

We studied the catalytic properties of the Pd and Au complexes in hydrogenation reactions in a 100-mL batch reactor (Autoclave Engineers) at 40 °C, 4 atm dihydrogen pressure, and a metal/substrate molar ratio of 1/1000. The evolution of the reaction of hydrogenated product was monitored by gas chromatography analysis using a Hewlett–Packard 5890 II with a flame ionization detector in a cross-linked methylsilicone column.

2.2. Catalyst recovery and recycling

At the end of the hydrogenation process, the mixture of reaction was filtered. The residue of the mesoporous support was washed to completely remove the remains of products and/or reactants and then reused.

2.3. Computational details

Calculations were carried out using the program package Gaussian03 [23] at a density functional theory (DFT) level using the hybrid B3LYP functional [24]. The basis set for N and O was 6-31g(d), that for Cl was 6-31 + g(d), that for C and H directly involved in the reaction was 6-31g(d,p), and that for the rest of the C and H atoms was 6-31g. The Pd was described by means of the LANL2DZ [25] pseudopotential and its associated basis set for the valence electrons. Solvent effects were included by means of the polarized continuum model (PCM) [26].

For the transition states, analytical frequencies were calculated to ensure that only 1 imaginary value was obtained. Normal coordinate analyses were performed on these saddlepoints by intrinsic reaction coordinate (IRC) routes [27] in both directions to the corresponding minima. When the IRC calculations did not converge, additional geometry optimizations starting from the IRC structures were carried out to identify the reactants and products linked by the specific TS considered.

3. Results and discussion

3.1. Synthesis and characterization of ligands and complexes

In recent years, we have developed a modular system combining functionalized ligands with different supports and linkers, to allow systematic access to various immobilized chiral catalysts [28]. Here we applied this methodology to immobilize the Schiff base ligand **2** (see Scheme S3 in Supplementary material) on a mesoporous silica support such as MCM-41.

Table 1
Turnover frequencies (TOF, h^{-1}),[a] for the catalytic hydrogenation of diethyl itaconate in EtOH[b]

Ligand	Au^{III}	Pd^{II}
2	3430	3360
2-(MCM-41)	4920	4980
2-(MCM-41, Si/Al = 50)	6730	6000

[a] TOF = $mmol_{subs.}/mmol_{cat.}$ h.
[b] 4 bar H_2, 40 °C and substrate/catalyst ratio 1000.

MCM-41 is a short-range amorphous material containing a large number of silanol groups available for grafting, but has long-range ordering with hexagonal symmetry with regular monodirectional channels 3.5 nm in diameter.

All solids were functionalized in the same manner according to the procedure described in the Supplementary Material. Supported precursors, ligands, and heterogenized ligands were characterized by microanalysis, FT IR, and ^{13}C NMR. The heterogenized ligands reacted with palladium(II) acetate or tetrachloroauric acid to furnish the corresponding anchored Pd^{II} and Au^{III} complexes used for catalytic reactions. The catalysts prepared on this way presented metal loading of 0.10–0.30 $mmol_{metal}/g_{support}$ as determined by atomic absorption analysis and were characterized by various spectroscopic techniques (see Supplementary material).

3.2. Catalytic hydrogenation activity

The hydrogenation of diethyl ethylidensuccinates (i.e., diethyl itaconate, diethyl citraconate, and diethyl benzylidensuccinate) with these structurally well-defined Pd^{II} and Au^{III} complexes was carried out under mild conditions (EtOH as the solvent, 4 atm. hydrogen pressure, 40 °C). The hydrogenation was carried out to explore the possibilities of recovering the catalysts, the influence of the nature of the support, and the comparison of the activity and stability of supported catalysts with their homogeneous counterpart. The results for the hydrogenation of diethyl itaconate catalyzed by Pd^{II} and Au^{III} complexes are given in Table 1.

It can be seen that the activity of the homogeneous Au^{III} and Pd^{II} complexes is similar and, for both metals, the TOFs in the case of the supported catalysts increase with respect to the homogeneous systems. This indicates that silica mesostructured molecular sieves (MCM-41) are suitable supports for heterogenizing metal-complex homogeneous catalysts. Storage of the heterogenized catalysts at room temperature for 6 months had no effect on their catalytic performance, indicating that they are stable over time. They also were stable under reaction conditions and could be recycled at least 6 times with no appreciable loss in activity (Fig. 1).

It has been shown [20] that in the case of Au^{III}-catalyzed alkene hydrogenation, the hydrogen is activated through heterolytic cleavage to give a hydride intermediate. This process involves charge separation with no oxidative addition of hydrogen to the metal; thus, increasing polarity and acidity of the support should increase the reaction rate. To test this hypothesis, we supported complexes **2Au** and **2Pd** on pure silica

MCM-41 (a very polar support due to its numerous surface silanol groups) and on MCM-41 in the form of aluminosilicate (Si/Al = 15), which presents surface Brönsted acid sites. In both cases, the catalytic activity of the supported complexes increased with respect to the homogeneous systems, suggesting that the activation of H_2 by Pd^{II} is similar to that previously obtained for Au^{III} [22].

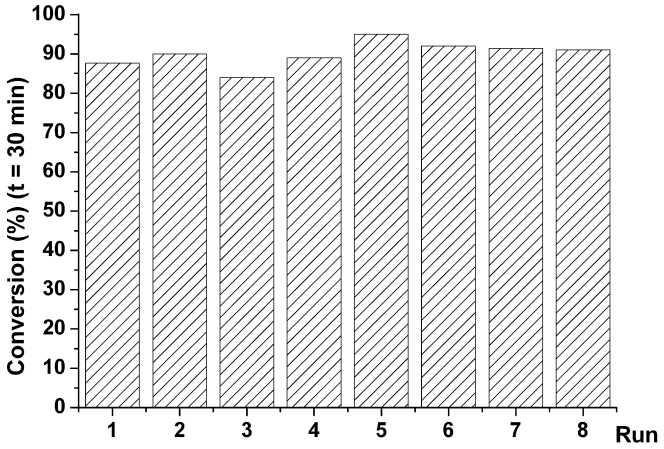

Fig. 1. Catalytic hydrogenation of diethyl itaconate with 2Pd-MCM-41.

We evaluated the influence of reaction temperature and H_2 pressure on the activity of the **2Pd** complex for hydrogenation of diethyl benzylidensuccinate; the results are shown in Fig. 2. As in the case of gold, the kinetic curves show an induction period that is more significant at low temperature; however, when the partial pressure of H_2 is varied from 2 to 4 bar, the induction period diminished for the **2Au** catalyst but did not change for the **2Pd** catalyst (Fig. 2b). With respect to the influence of the solvent used (depicted in Fig. 3), it is considerably greater in the case of gold. We discuss these effects and their causes throughout the article.

3.3. Reaction mechanism

According to the literature [29,30], the proposed mechanism of alkene hydrogenation catalyzed by Pd^{II} complexes comprises 3 main steps, which we describe in this section: (i) initial activation of the dihydrogen molecule, (ii) incorporation of the alkene into the coordination sphere of the catalyst and inser-

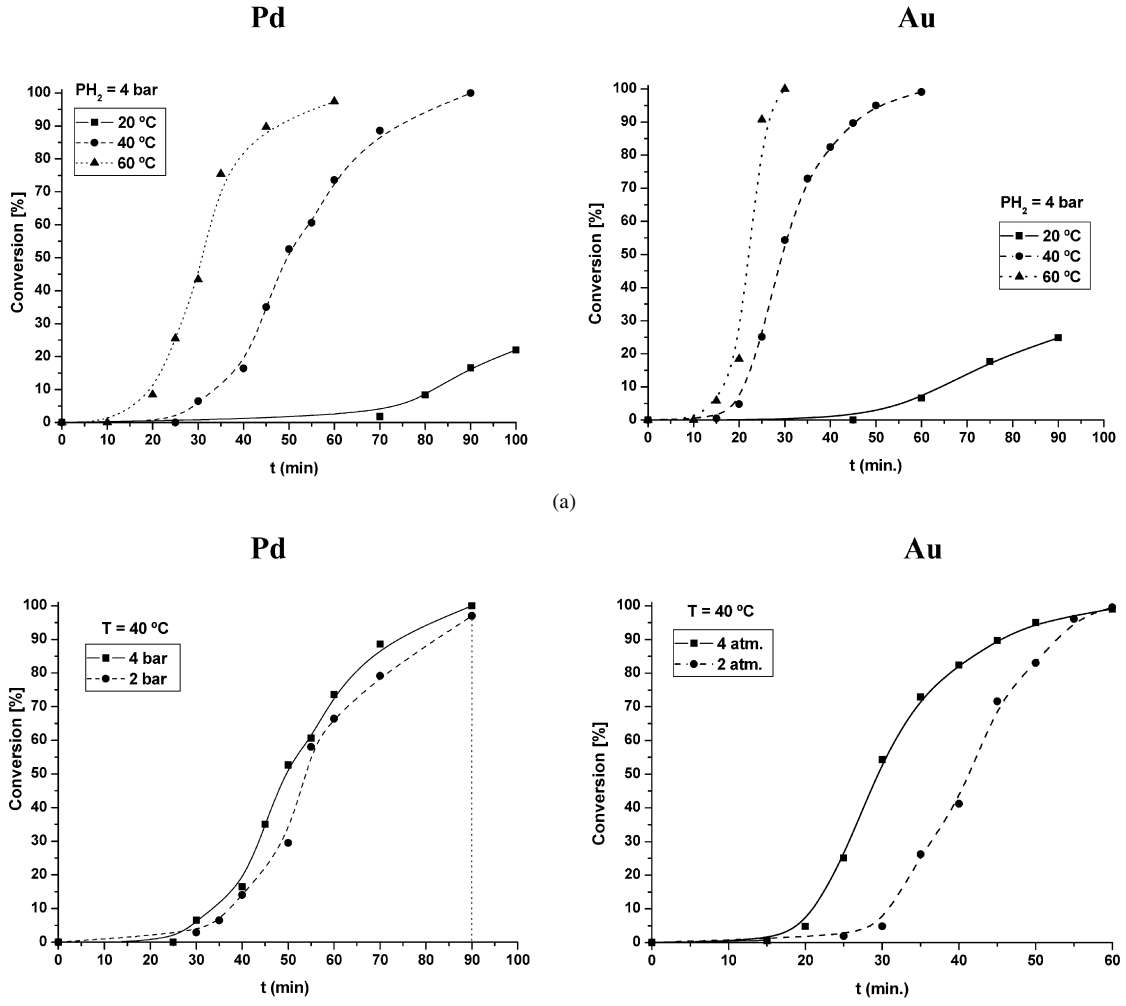

Fig. 2. Hydrogenation of diethyl benzylidensuccinate using **2Pd** (left) and **2Au** (right) catalysts and ethanol as solvent. Influence of (a) reaction temperature and (b) H_2 pressure.

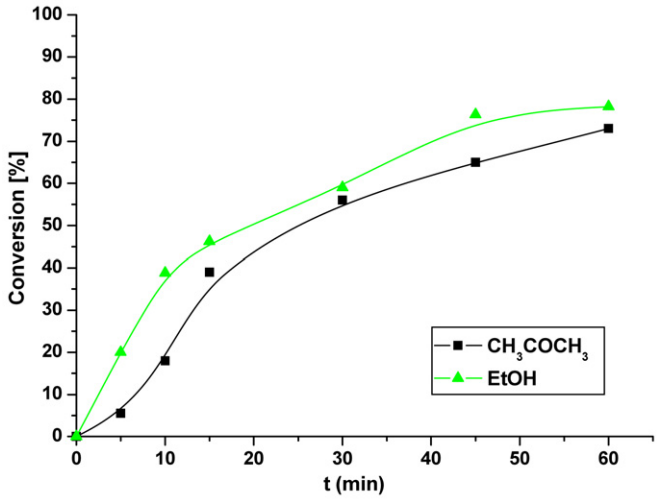

(a)

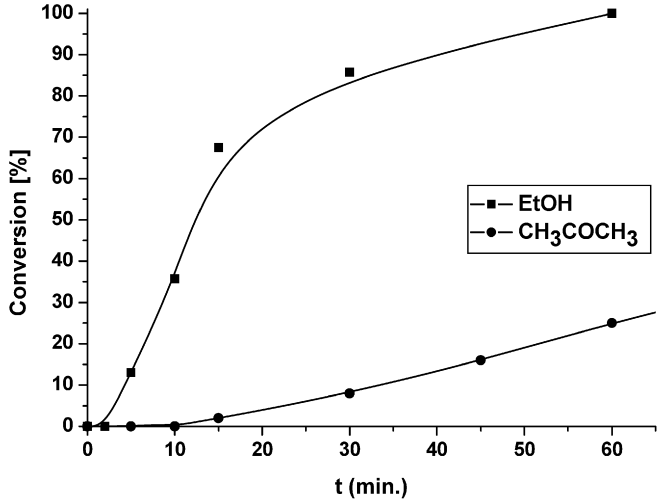

(b)

Fig. 3. Influence of solvent on the hydrogenation of diethyl benzylidensuccinate using (a) **2Pd** and (b) **2Au** catalysts.

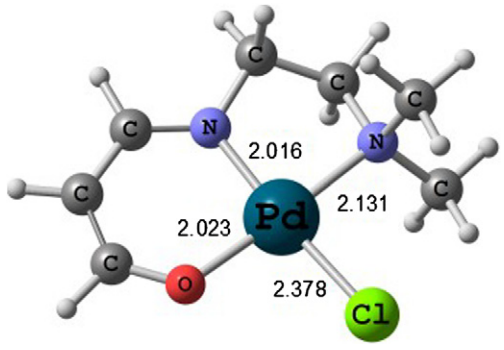

Fig. 4. Model complex for the catalyst. Distances in Å.

tion into the Pd–H bond, and (iii) a second hydrogen transfer closing the catalytic cycle. The mechanism of the reaction catalyzed by **2Pd**, as shown in Scheme S3 in the Supplementary material, was calculated using the complex depicted in Fig. 4 as a model for the catalyst and ethylene as the simplest alkene. We next discuss the results obtained for these 3 main steps.

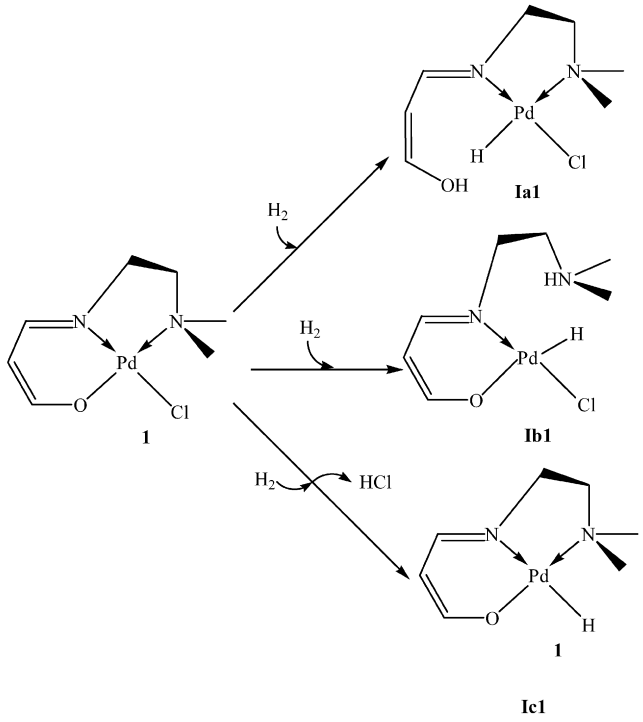

Fig. 5. Possible heterolytic cleavage pathways for the dihydrogen molecule.

3.3.1. *Activation of the H_2 molecule*

Because the hydrogen source in the present reaction was molecular hydrogen, the H_2 molecule had to be activated by the metallic complex to perform alkene hydrogenation. Two known routes are available for activating the dihydrogen molecule: homolytic cleavage and heterolytic cleavage. As discussed previously, the influence of the support on the activity of Pd^{II} complexes (similar to that of Au^{III}), along with the difficulty that the metal center has in reaching the oxidation number Pd^{IV}, make homolytic activation of the dihydrogen molecule highly improbable for this complex. This is commonly accepted for Pd(II) hydrogenation catalysts [29–31]. This was indeed confirmed by theoretical calculations; the product of the oxidative addition was found to lay 37.9 kcal/mol above that of the reactants, indicating that the barrier for this reaction will be at least 37.9 kcal/mol. Thus, we discounted homolytic cleavage as a possible pathway for H_2 activation.

H_2 heterolytic cleavage is more common in early-transition metals, even though several cases have recently been reported for late-transition metals [32–39]. For this particular system, the catalyst had several ligands that were able to undergo $[2+2]$ σ bond metathesis of the dihydrogen molecule: the oxygen and nitrogen of the Schiff base ligand and the chlorine ligand. In all of these pathways (depicted in Fig. 5), the hydrogen molecule is heterolytically activated by the catalyst; a proton goes to the ligand, whereas a hydride is bonded to the metal, keeping the oxidation state of Pd unchanged. The participation of hydride palladium species in hydrogenation reactions has been proposed previously [40,41].

A previous computational study of alkene hydrogenation catalyzed by Au^{III} complexes [20] found the highest barrier in the pathway in which activation occurs by means of the

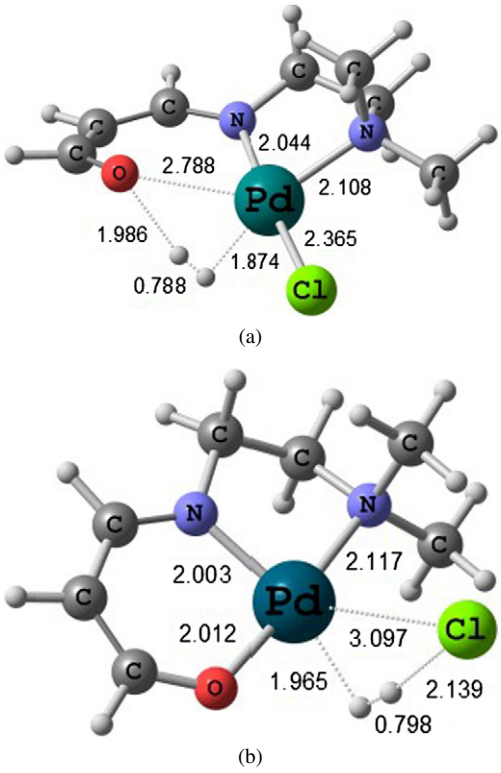

Fig. 6. Optimised geometry of the transition states for the heterolytic cleavage of H_2: (a) over the O ligand (**ts1a**) and (b) over the Cl ligand (**ts1c**). Distances in Å.

N(amine) ligand. In addition, the N(amine) ligand can be easily replaced by the olefin within the catalytic cycle (vide infra). Thus, in the case of the Pd catalyst, we did not consider this possibility for hydrogen activation, and performed calculations for the heterolytic cleavage only over O and Cl ligands.

Heterolytic cleavage over the O atom presented a barrier of 32.0 kcal/mol in the gas phase. Including solvent effects, the barrier remained practically unchanged, with a value of 32.7 kcal/mol. Referring to the possibility of dihydrogen splitting over the chlorine atom in the gas phase, the barrier was 28.1 kcal/mol with respect to the corresponding reactants, in which the hydrogen molecule is weakly interacting with the catalyst. In this case, however, the barrier height decreased significantly when solvent effects were included through a continuum model, adopting a value of 19.2 kcal/mol. The transition states for the heterolytic cleavage of H_2 over O and Cl are shown in Fig. 6, and the variation in the Mulliken charges on selected atoms in relation to separated reactants is given in Table 2. In the case of H_2 splitting over O (**ts1a**), the Pd center decreased its positive charge considerably, whereas the O atom did not significantly change its negative charge, because the oxygen atom can delocalize the charge over the adjacent π system. In contrast, in the case of H_2 cleavage over Cl (**ts1c**), there was a considerable increase in the negative charge on the chlorine atom, indicating that the polarity of the solvent (ethanol) played a significant role in this case, decreasing the activation barrier by about 9 kcal/mol.

In the case of the analogous Au^{III} catalyst [20], as well as in other samples reported by other authors using different catalysts [39], it was shown that the participation of species with proton donor-acceptor capabilities could significantly modify the reaction energy profiles. Therefore, we focused our efforts on searching for a reaction step in which a solvent molecule (ethanol) is directly implicated in the heterolytic activation of H_2. The optimized structures of the solvent-assisted transition states obtained over both the oxygen and the chlorine ligand atoms are depicted in Fig. 7.

Table 2
Variation in the Mulliken calculated atomic charges on selected atoms in relation to separated reactants in the gas phase (g) and with the solvent included by means of the PCM method (PCM)

	ts1a (g)	**ts1a** (PCM)	**ts1c** (g)	**ts1c** (PCM)
Pd	−0.214	−0.227	0.089	0.073
Cl	0.067	0.089	−0.321	−0.314
O	0.015	0.007	−0.004	0.002

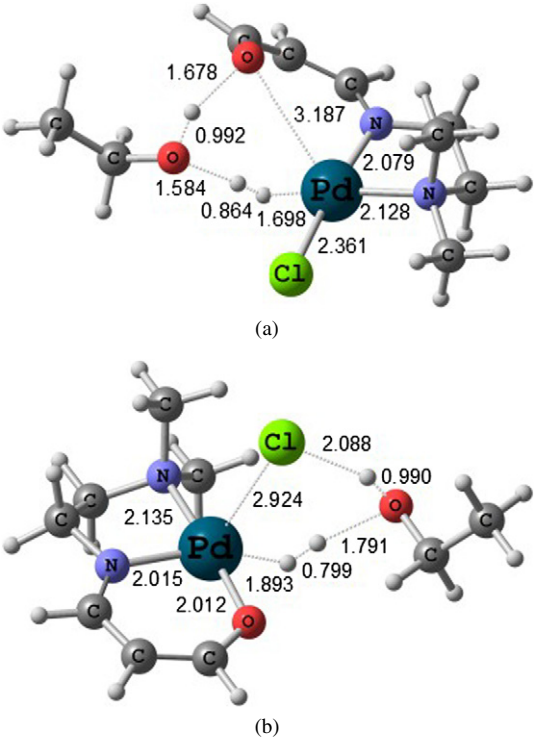

Fig. 7. Optimised geometry of the transition states for the solvent-assisted heterolytic cleavage of H_2: (a) over the O ligand (**ts1a2**) and (b) over the Cl (**ts1c2**). Distances in Å.

The geometry of these transition states can be associated with a trigonal bipyramid structure in which the leaving ligand and the forming hydride both lay at the equatorial plane. The barrier heights of these steps are 32.8 for O and 18.6 kcal/mol for Cl, practically equivalent to those calculated for the non-solvent-assisted process. These results indicate that, as in the Au^{III} complex, the heterolytic activation of H_2 was far more favorable over the chlorine atom than over the oxygen atom. Nevertheless, in contrast to the Au^{III} complexes, the direct assistance of a solvent molecule did not significantly decrease the activation barrier for the H_2 heterolytic splitting. Fig. 3 compares the influence of the solvent on the activity of Au^{III} and Pd^{II} complexes as determined experimentally. For Pd^{II}, the ac-

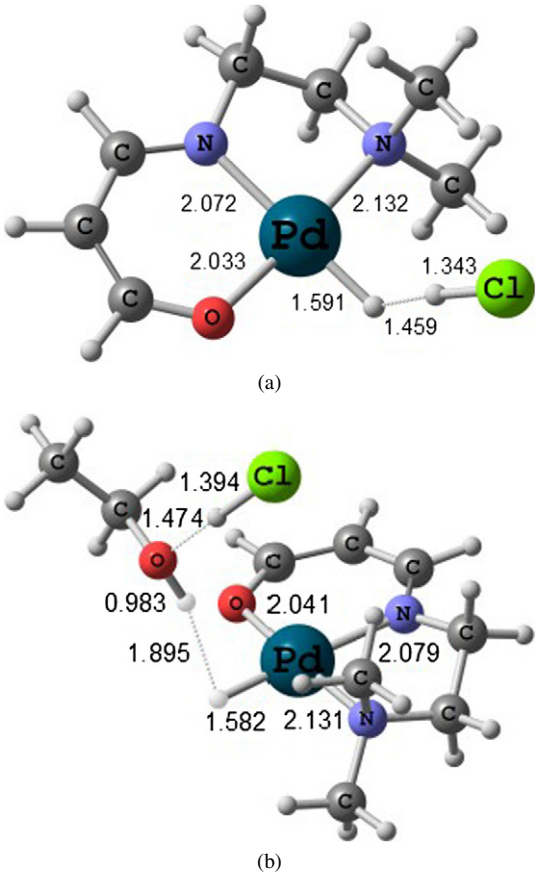

Fig. 8. Products of the heterolytic splitting of the dihydrogen molecule over the Cl ligand: (a) product for the non-assisted pathway (**Ic1–HCl**), (b) product of the assisted pathway (**Ic1–EtOH**). Distances in Å.

tivity was slightly improved when ethanol was used instead of acetone; this may be related to the slightly higher polarity of ethanol (dielectric constant $\varepsilon = 24.55$) with respect to acetone ($\varepsilon = 20.70$) [42]. For Au^{III}, however, the effect of the solvent was much more pronounced, because the activity in ethanol was considerably higher than that in acetone. This effect cannot be explained only in terms of solvent polarity, but rather is related to the active role of the ethanol molecule in the heterolytic activation of H_2. According to the mechanism calculated for Au^{III} complexes, a solvent with proton-donating ability, such as ethanol, is required for the reaction to proceed.

Fig. 8 shows the optimized geometry of the products of the nonassisted and the solvent-assisted pathways for the **2Pd** catalyzed reaction. It can be seen that in the product of the heterolytic cleavage without solvent assistance, a dihydrogen bond exists between the hydride of the Pd–H bond and the proton of the recently formed HCl molecule characterized by a distance of 1.459 Å (**Ic1–HCl**). This product is located at 18.8 kcal/mol with respect to the catalyst and the hydrogen molecule. The solvent-assisted heterolytic cleavage of the dihydrogen molecule produced an intermediate in which the proton of the HCl molecule was hydrogen-bonded with the oxygen atom of the ethanol molecule (**Ic1–EtOH**). This hydrogen bond is strong, with a distance of 1.474 Å. In this product, the proton of the ethanol molecule forms a dihydrogen bond with the hydride

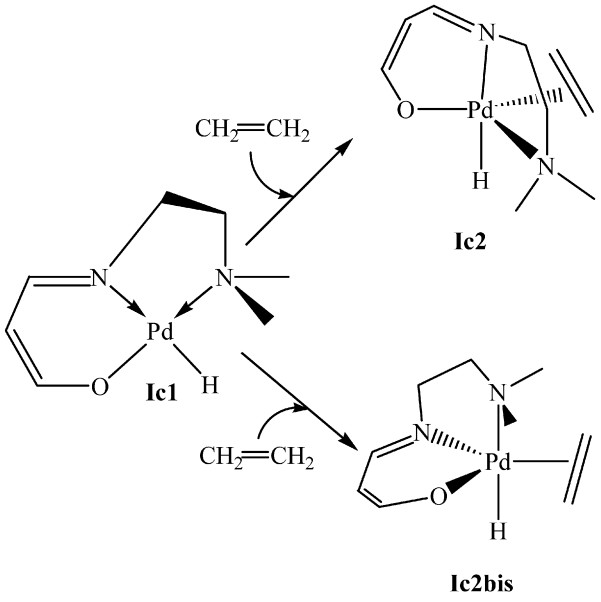

Fig. 9. Trigonal bipyramid structures after ethylene coordination.

ligand [43], with a H–H distance of 1.895 Å. This product is located 12.5 kcal/mol above the respective reactants: H_2, ethanol, and the catalyst interacting. It should be noted that in the analogous process in gold catalysis this step was exothermic by more than 10 kcal/mol [20]. This difference is likely due to the fact that the Au^{III} catalyst was positively charged, and the products in that case were $EtOH_2^+$ and Cl^- forming an ionic pair.

Based on the foregoing results, we can conclude that when Pd^{II} complexes are used as catalysts, the dihydrogen heterolytic cleavage is more favorable over chlorine than over the oxo group. Our calculations also indicate, in agreement with experimental evidence, that although solvent effects are important in lowering the activation barrier, the direct assistance of a solvent molecule is not needed for the reaction to occur, in contrast with the results obtained for the Au^{III} catalysts.

3.3.2. *Coordination and insertion of the olefin to the catalyst*

The next step in the catalytic cycle involves the alkene molecule. Exploring the potential energy surface for a pentacoordinated structure including the alkene in the coordination sphere of the catalyst identified two isomers, **Ic2** and **Ic2bis**. These isomers exhibited geometry close to that of a trigonal bipyramid structure. The relative energies of **Ic2** and **Ic2bis** intermediates with respect to ethylene and **Ic1** were 14.6 and 14.9 kcal/mol, respectively. These two structures are schematically represented in Fig. 9, and their optimized geometries are depicted in Fig. 10.

In principle, the reaction could evolve from any of these isomers. Therefore, we examined a reaction pathway starting from each of these intermediates. The two pathways found for olefin insertion into the Pd–H bond are schematically depicted in Fig. 11. From the **Ic2** intermediate, the reaction may evolve through ligand coordination breaking to regenerate a square planar structure, with the alkene occupying the position previously occupied by the N(amine) ligand. The optimized geometry of the transition state for this step (**ts2**) is depicted in Fig. 12.

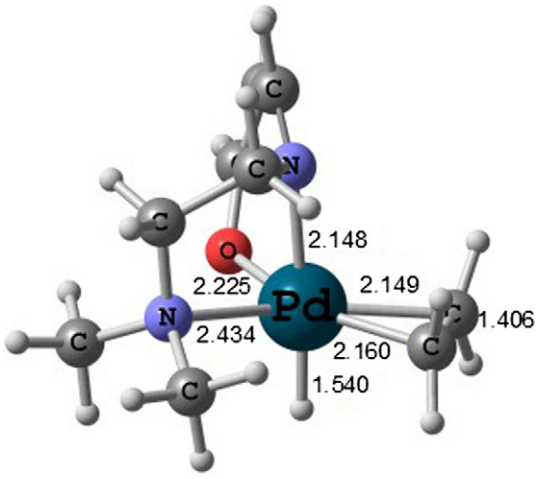

(a)

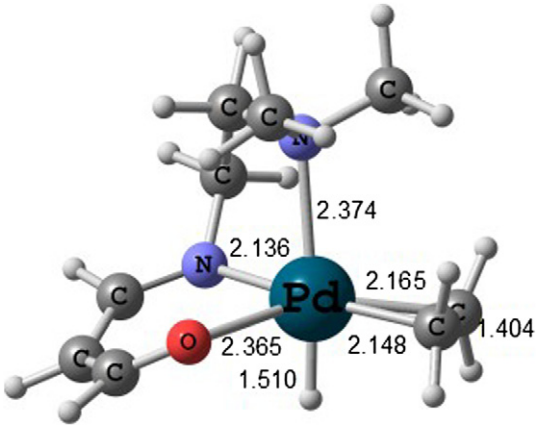

(b)

Fig. 10. Optimised geometry of the trigonal bipyramid isomers: (a) **Ic2** and (b) **Ic2bis**. Distances in Å.

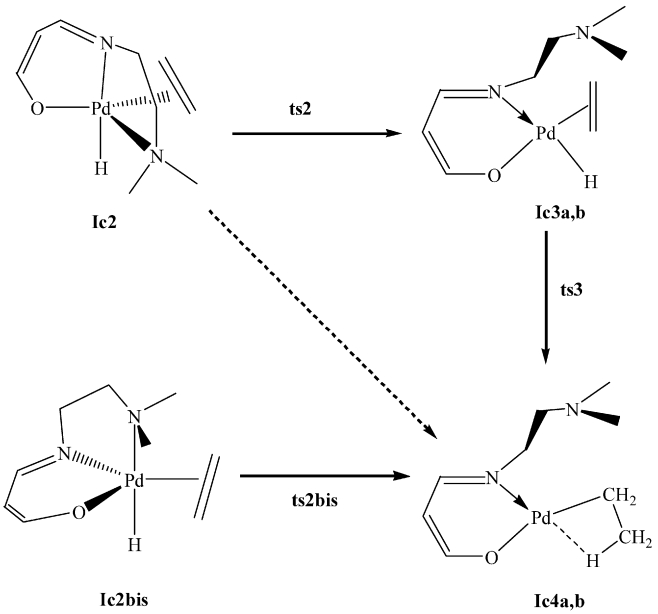

Fig. 11. Different pathways to obtain the alkyl intermediate (**Ic4a,b**) from **Ic2** and **Ic2bis**.

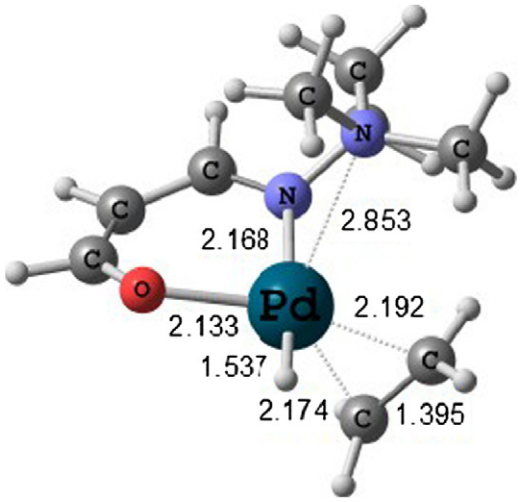

(a)

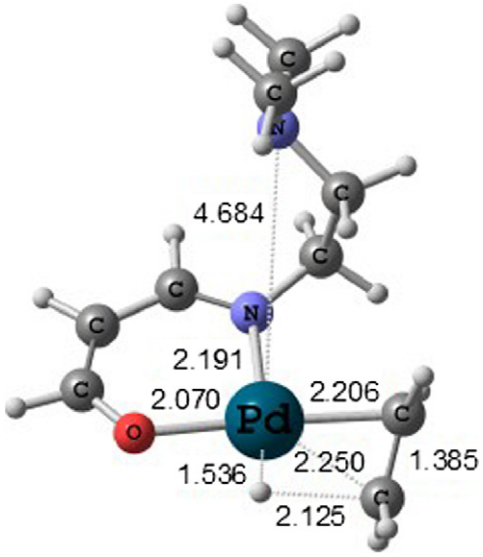

(b)

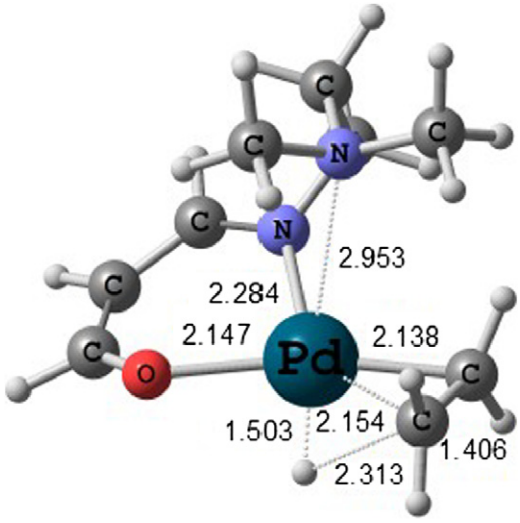

(c)

Fig. 12. Optimised geometry of the transition states for (a) ethylene coordination with N(aminic) leaving (**ts2**), (b) ethylene insertion into the Pd–H bond after N(aminic) leaving (**ts3**) and (c) N(aminic) leaving and ethylene insertion into the Pd–H bond occurring concomitantly (**ts2bis**). Distances in Å.

The energy cost for N(amine) removal and ethylene coordination starting from **Ic2** was only 0.4 kcal/mol, and formation of the **Ic3a** intermediate was exothermic by 6.3 kcal/mol. A related study by Vrieze and co-workers [44] on the insertion reaction of CO into Pd–C bonds of complexes containing terdentate nitrogen ligands proposed that one of the terminal N of the chelate ligand is substituted by the incoming CO within the reaction mechanism [44]. Another study in a different system analogously proposed the breakage of one labile palladium–pyridine bond in alkyne hydrogenation to coordinate an additional molecule present in the reaction media, such as hydrogen or an alkyne molecule [45].

Once the square planar intermediate **Ic3a** is formed, a small conformational change (associated to the change of the N–C–C–N dihedral angle) gives rise to intermediate **Ic3b,** which is lower in energy (by 0.6 kcal/mol). In both intermediates **Ic3a** and **Ic3b**, coordination of the olefin is perpendicular to the plane containing the metal center and the other ligands. The next step corresponds to insertion of the alkene into the Pd–H bond through transition state **ts3**. This process has been systematically studied computationally for the second-row metal complexes, including a palladium monohydride species [46]. The insertion process involves rotation of the olefin concomitantly to the insertion process itself (see Fig. 12b), producing the intermediate **Ic4a**, in which there is an agostic interaction between the metal and the recently formed C–H bond, as expected after the insertion process [47a]. This step is thermodynamically favorable by 8.8 kcal/mol, with an energy barrier of 5.0 kcal/mol. Along with **Ic4a,** there is another conformer, **Ic4b**, which is 0.8 kcal/mol lower in energy.

An alternative pathway for forming the intermediate **Ic4b** starts from the **Ic2bis** structure. In this case, the process occurs in a single step; the transition state **ts2bis** reveals a simultaneous hydride migration to the ethylene molecule and breaking of the coordination of the N(amine) ligand. The energy barrier for this process is 9.6 kcal/mol. This pathway is energetically less favorable than the two-step pathway starting form the **Ic2** intermediate, in which the highest barrier is 5.0 kcal/mol. These results are in agreement with the conclusion reached by Thorn and Hoffmann [48] that ethene insertion into a M–H bond is more difficult in a trigonal bipyramidal structure than in a square planar structure [48].

The existence of direct hydride migration concomitantly with the N(amine) leaving when starting from the **Ic2bis** structure led us to consider an analogous process starting from the **Ic2** structure (see the dashed arrow in Fig. 11). Although we extensively searched this direct process in the potential surface, we could not locate the associated transition state. In any case, this process is expected to be energetically similar to that starting from **Ic2bis**, which is higher than the stepwise process previously shown.

3.3.3. Second hydrogen transfer closing the catalytic cycle

The next step in the proposed reaction mechanism is the second hydrogen transfer process yielding the product, ethane. The possibility of alkyl protonation by the acid formed in the first step, as suggested in the literature [30,31], has been analyzed

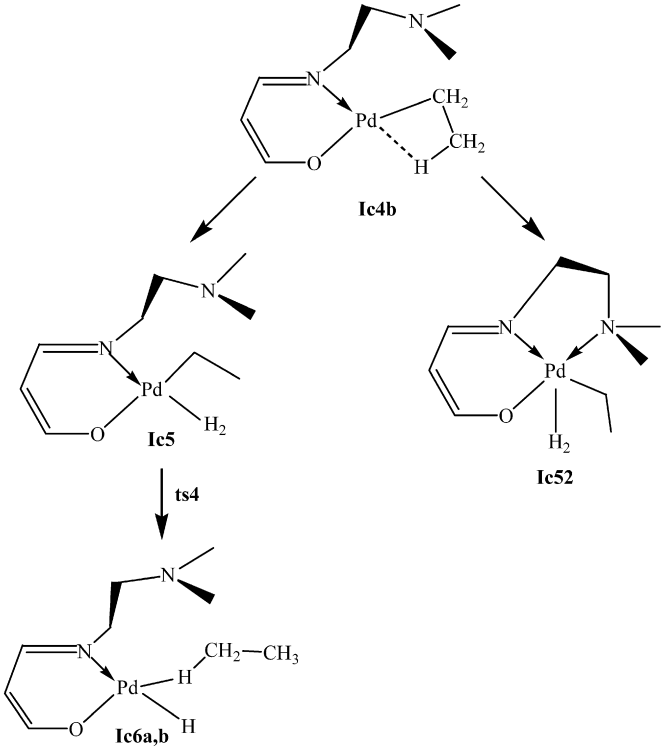

Fig. 13. Different ways of coordination of H_2 to the **Ic4b** intermediate and evolution of **Ic5**.

for the Au^{III} system and found to be energetically prohibitive [20]; therefore, we did not consider this pathway here. Instead, we investigated H_2 molecule coordination to the catalyst at intermediate **Ic4b**. The two alternatives considered for this H_2 coordination are shown in Fig. 13. In the first of these, the **Ic4b** intermediate evolves by breaking the weak agostic interaction between the metal and the C–H bond and coordinating the dihydrogen molecule into the vacant site forming the **Ic5** intermediate, an exothermic process by 4.0 kcal/mol. In the second pathway, the N(amine) of the Schiff base complex coordinates again to the vacant site and H_2 coordinates to the complex, forming a penta-coordinated structure, **Ic52**. Extensive exploration of the potential energy surface around the coordination mode supposed for the **Ic52** intermediate was performed without success; thus, calculations suggest that when it exists, this penta-coordinated intermediate will be very high in energy.

Consequently, the reaction mechanism was considered to go through intermediate **Ic5**. After the dihydrogen molecule coordination, the next step corresponds to hydrogenolysis to give the hydride intermediate **Ic6a** (see Fig. 13) and ethane, which remains coordinated to the complex by means of an agostic interaction between the metal and one of the C–H bonds. H_2 activation goes through a four-centered metathesis-like transition state (**ts4** in Fig. 14) with an activation energy of 12.1 kcal/mol. An analogous hydrogenolysis step also has been found to be favorable for the chain termination process in ethylene polymerization by means of the diimine–palladium [47b] and diimine–nickel [47c], and also in a hydride-exchange process [49].

The final step in the catalytic cycle involves the conformational change of a side chain of the N(amine) ligand, fa-

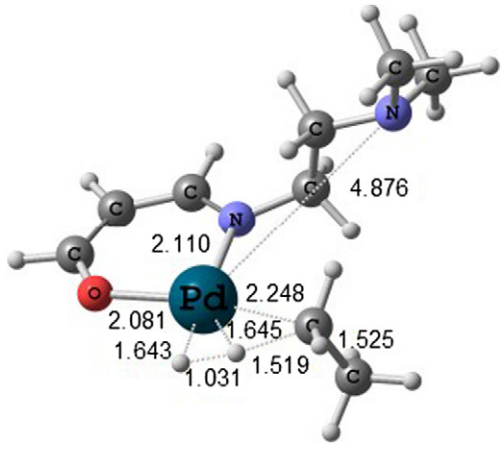

Fig. 14. Optimised geometry of the transition state for the hydrogenolysis of H_2 (**ts4**). Distances in Å.

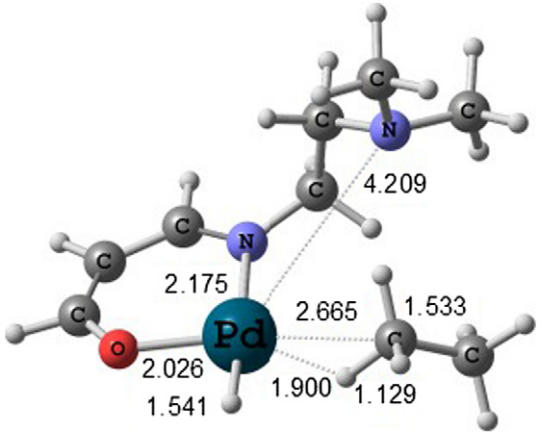

(a)

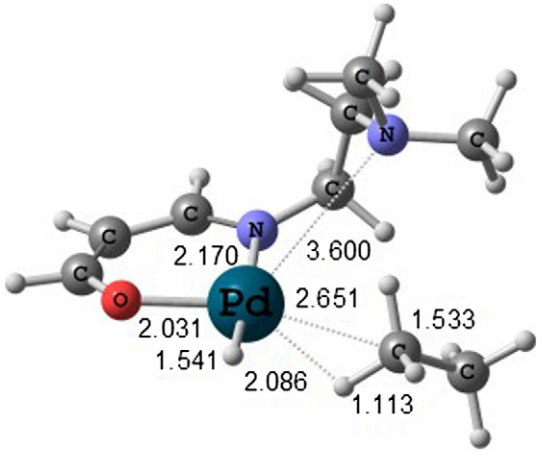

(b)

Fig. 15. Optimised geometry of the transition states for (a) conformational change of the aminic chain (**ts5**) and (b) N(aminic) coordination to Pd with ethane release occurring concomitantly (**ts6**). Distances in Å.

cilitating its coordination to palladium, concomitantly with product (ethane) release. The conformational change of the aminic chain (producing intermediate **Ic6b**) has a barrier height of 2.9 kcal/mol, and the process is endothermic by only 2.3 kcal/mol. The optimized geometry of the transition state for this process, **ts5**, is shown in Fig. 15. The simultaneous co-

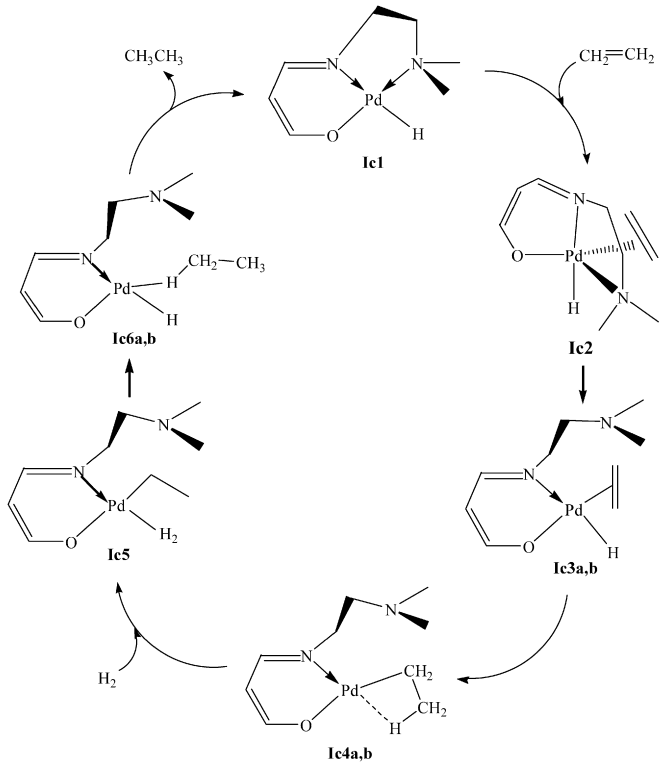

Fig. 16. Proposed catalytic cycle without the initial H_2 activation. Letters written after the intermediate labels correspond to different conformers of the same species.

ordination of the N(amine) ligand and the elimination of the ethane molecule through transition state **ts6** (see Fig. 15) has a barrier of only 0.2 kcal/mol. Moreover, this step is exothermic by 33.3 kcal/mol and regenerates the palladium–hydride intermediate **Ic1**, thereby providing an elegant and easy way to close the catalytic cycle. Actually, the final product is a different conformer of the hydride species. Both conformers (see the initial and final catalysts of the energy profile in Fig. 17) are isoenergetic; thus, they have not been distinguished, and both are referred to as **Ic1** in the present work.

3.4. Global reaction mechanism

The complete catalytic cycle, without initial H_2 activation and simplifying some steps that involve conformational rearrangements, is shown in Fig. 16, and the corresponding energy profile is depicted in Fig. 17. The highest energy barrier of the proposed mechanism is 19.2 kcal/mol, which corresponds to the initial activation of H_2 through its heterolytic cleavage over the chlorine ligand. Nevertheless, this process is not within the catalytic cycle; once the hydrogen molecule has been initially activated forming the palladium–hydride intermediate, **Ic1**, this is the active species involved in the catalytic cycle. This should result in an induction period in the kinetic curve, which indeed has been observed experimentally. In Fig. 2a, it can be seen that the induction period is more significant at low temperature and is slightly diminished when the partial pressure of H_2 is increased from 2 to 4 bar (Fig. 2b).

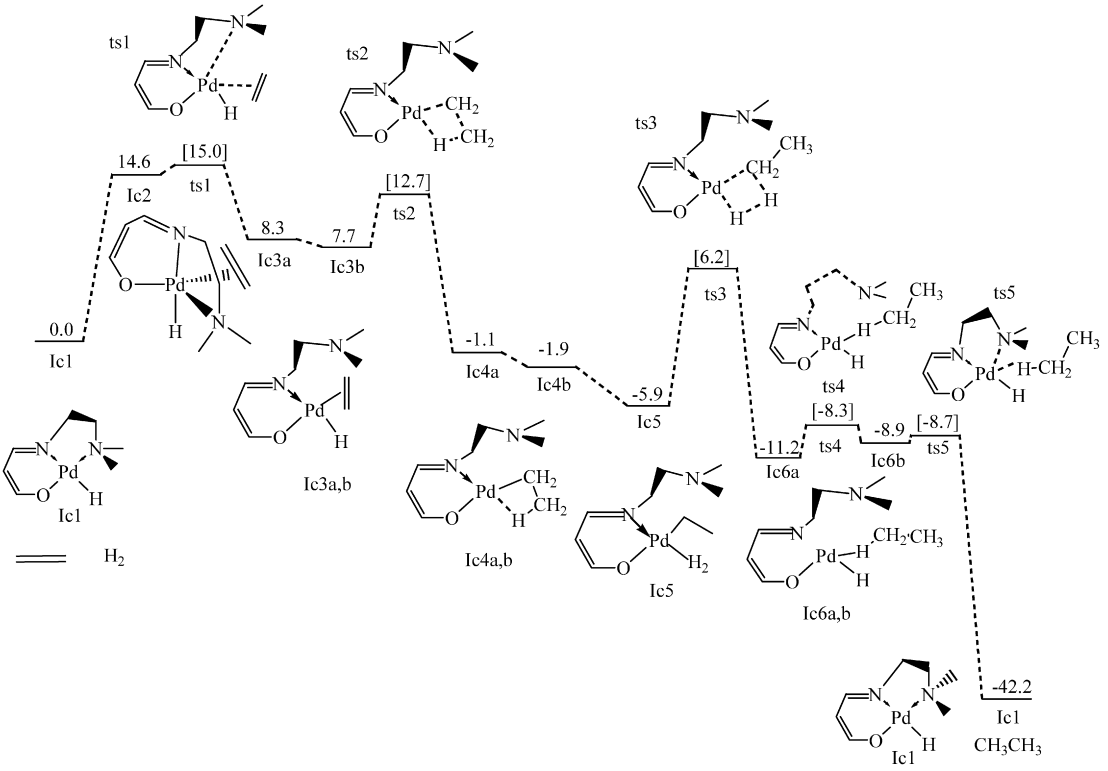

Fig. 17. Calculated energy profile for the proposed mechanism. Energies in kcal/mol.

The second activation of the H_2 molecule, which occurs within the catalytic cycle, occurs in a different (and easier) manner. In this case, the H_2 molecule initially coordinates to a vacant site in the Pd catalyst before undergoing the hydrogenolysis process, which has a lower energy barrier (12.1 kcal/mol). The highest energy barrier step in the catalytic cycle corresponds to N(amine) ligand substitution by the incoming ethylene molecule. This process implies initial ethylene coordination to the catalyst; a new ligand is added to the palladium catalyst, forming a penta-coordinated structure—a process not favorable for a metal center with d^8 electronic configuration. The next step implies N(amine) descoordination to generate again a square planar structure, with an activation barrier of 15.0 kcal/mol for the overall process. Concerning the solvent effects, calculations indicate that its inclusion in the Pd^{II}-catalyzed reaction is important because the energy barrier of the initial step is significantly diminished. Nevertheless, and conversely to the analogous Au^{III} catalyst, in this case both theoretical and experimental results suggest that solvent plays no active role in the reaction mechanism.

4. Conclusion

In the present work, the catalytic performance and the reaction mechanism of a homogeneous and two heterogenized Schiff base complexes of Pd^{II} and Au^{III} in the hydrogenation reactions of diethyl ethylidensuccinates have been analysed and compared by means of kinetic and computational studies. The reaction mechanism for the Pd^{II} catalyst occurs in three main steps: (i) heterolytic activation of hydrogen molecule, generating a Pd–hydride intermediate, (ii) coordination and insertion of the olefin into the catalyst, and (iii) coordination of H_2 molecule, proton transfer to substrate, and regeneration of the Pd–hydride species. Our results demonstrate that the hydrogenation mechanism using Pd^{II} complexes is similar to that of the Au^{III} counterparts, with some significant differences.

For the Pd^{II} complexes, the dihydrogen heterolytic cleavage is more favorable over chlorine than over the oxo group, as for the Au^{III} complexes. Calculations also indicate, in agreement with experimental evidence, that solvent effects are important to speeding-up the reaction rate. Nevertheless, in contrast to the Au^{III} complex, for the Pd^{II} complexes the direct assistance of a solvent molecule does not significantly decreases the energy barrier for the initial heterolytic activation of the hydrogen molecule. This fact is experimentally confirmed by the similar induction periods found for both acetone and ethanol solvents (conversely to the Au^{III} complex).

Regarding the rate-determining step, it is the same for both complexes once the catalytically active species (the hydride intermediate) is formed. This step corresponds to the coordination of the olefin to the catalyst. Nevertheless, whereas for the Pd^{II} complex, the addition of olefin built a pentacoordinated species, for the Au^{III} complex, no five-coordinated complex was found in the reaction mechanism.

The catalytic experiments on the hydrogenation of ethylidensuccinates for the homogeneous catalysts showed similar activity for Pd^{II} and Au^{III}. The TOFs for the supported catalysts increased compared with those for the homogeneous systems for both metals. The hydrogen molecule was heterolytically activated by the metal complex with no oxidative addition

process. This route implies a charge separation that should be facilitated by polar supports, as in fact was noted in the heterogenized catalysts.

Acknowledgments

Financial support for this work was provided by the Spanish MEC (projects MAT2003-07945-C02-01 and -02, and CTQ2005-09000-C02-01, a "Ramón y Cajal" contract to G.U. and FPU fellowships to A.C.-V.), as well as the Auricat EU Network (HPRN-CT-2002-0174), and Generalitat de Catalunya (2005/SGR/00896).

Supplementary material

The online version of this article contains additional supplementary material.

Please visit DOI: 10.1016/j.jcat.2007.12.015.

References

[1] P.N. Rylander, Catalytic Hydrogenation over Platinum Metals, Academic Press, New York, 1967.
[2] A. Yamamato, Organotransition Metal Chemistry, Wiley, New York, 1986.
[3] W.A. Herrmann, B. Cornils, Angew. Chem. Int. Ed. 36 (1997) 1048.
[4] M. Kram, Adv. Catal. 29 (1980) 151.
[5] Z.M. Michalska, D.E. Webster, CHEMTECH 5 (1975) 117.
[6] P.A. Chaloner, M.A. Esteruelas, F. Joó, L.A. Oro, Homogeneous Hydrogenation, Kluwer, Dordrecht, 1994.
[7] G. Dyker, Angew. Chem. Int. Ed. 39 (2000) 4237, and references therein.
[8] (a) G.J. Hutchings, S. Carrettin, P. Landon, J.K. Edwards, D. Enache, D.W. Knight, Y.J. Xu, A.F. Carley, Top. Catal. 38 (2006) 223;
(b) A.S.K. Hasmi, G.J. Hutchings, Angew. Chem. Int. Ed. 45 (2006) 7896.
[9] (a) X. Yao, Ch.-J. Li, J. Am. Chem. Soc. 126 (2004) 6884;
(b) Ch. Wei, Ch.-J. Li, J. Am. Chem. Soc. 125 (2003) 9584.
[10] M. Haruta, Catal. Today 36 (1997) 153.
[11] J. Guzman, B.C. Gates, J. Phys. Chem. B 106 (2002) 7659;
J. Guzman, B.C. Gates, J. Am. Chem. Soc. 126 (2004) 2672.
[12] M. Valden, X. Lai, D.W. Goodman, Science 281 (1998) 1647.
[13] J. Guzman, S. Carrettin, A. Corma, J. Am. Chem. Soc. 127 (2005) 3286.
[14] Q. Fu, H. Saltsburg, M. Flytzani-Stephanopoulos, Science 301 (2003) 935.
[15] A. Abad, P. Concepción, A. Corma, H. García, Angew. Chem. Int. Ed. 44 (2005) 4066.
[16] F. Porta, L. Prati, M. Rossi, G. Scari, J. Catal. 211 (2002) 464.
[17] S. Carrettin, J. Guzman, A. Corma, Angew. Chem. Int. Ed. 44 (2005) 2242.
[18] A. Corma, P. Serna, Science 313 (2006) 332.
[19] (a) C. González-Arellano, A. Corma, M. Iglesias, F. Sánchez, J. Catal. 238 (2006) 497;
(b) C. González-Arellano, A. Corma, M. Iglesias, F. Sánchez, Chem. Commun. (2005) 3451.
[20] A. Comas-Vives, C. González-Arellano, A. Corma, M. Iglesias, F. Sánchez, G. Ujaque, J. Am. Chem. Soc. 128 (2006) 4756.
[21] C. González-Arellano, E. Gutiérrez-Puebla, M. Iglesias, F. Sánchez, Eur. J. Inorg. Chem. (2004) 1955.
[22] C. González-Arellano, A. Corma, M. Iglesias, F. Sánchez, Adv. Synth. Catal. 346 (2004) 1316.
[23] M.J. Frisch, G.W. Trucks, H.B. Schlegel, G. Scuseria, M.A. Robb, J.R. Cheeseman Jr., J.A. Montgomery, T. Vreven, K.N. Kudin, J.C. Burant, J.M. Millam, S.S. Iyengar, J. Tomasi, V. Barone, B. Mennucci, M. Cossi, G. Scalmani, N. Rega, G.A. Petersson, H. Nakatsuji, M. Hada, M. Ehara, K. Toyota, R. Fukuda, J. Hasegawa, M. Ishida, T. Nakajima, Y. Honda, O. Kitao, H. Nakai, M. Klene, X. Li, J.E. Knox, H.P. Hratchian, J.B. Cross, V. Bakken, C. Adamo, J. Jaramillo, R. Gomperts, R.E. Stratmann, O. Yazyev, A.J. Austin, R. Cammi, C. Pomelli, J.W. Ochterski, P.Y. Ayala, K. Morokuma, G.A. Voth, P. Salvador, J.J. Dannenberg, V.G. Zakrzewski, S. Dapprich, A.D. Daniels, M.C. Strain, O. Farkas, D.K. Malick, A.D. Rabuck, K. Raghavachari, J.B. Foresman, J.V. Ortiz, Q. Cui, A.G. Baboul, S. Clifford, J. Cioslowski, B.B. Stefanov, G. Liu, A. Liashenko, P. Piskorz, I. Komaromi, R.L. Martin, D.J. Fox, T. Keith, M.A. Al-Laham, C.Y. Peng, A. Nanayakkara, M. Challacombe, P.M.W. Gill, B. Johnson, W. Chen, M.W. Wong, C. Gonzalez, J.A. Pople, Gaussian 03, Revision C.02, Gaussian, Inc., Wallingford, CT, 2004.
[24] (a) A.D. Becke, J. Chem. Phys. 98 (1993) 5648;
(b) C. Lee, W. Yang, R.G. Parr, Phys. Rev. B 37 (1998) 785;
(c) P.J. Stephens, J.F. Devlin, C.F. Chabalowski, M.J. Frisch, J. Phys. Chem. 98 (1994) 11623.
[25] P.J. Hay, W.R. Wadt, J. Chem. Phys. 82 (1985) 270.
[26] (a) M.T. Cancès, B. Mennucci, J. Tomasi, J. Chem. Phys. 107 (1997) 3032;
(b) M. Cossi, V. Barone, B. Mennucci, J. Tomasi, Chem. Phys. Lett. 286 (1998) 253;
(c) B. Mennucci, J. Tomasi, J. Chem. Phys. 106 (1997) 5151.
[27] (a) K. Fukui, Acc. Chem. Res. 14 (1981) 363;
(b) C. Gonzalez, H.B. Schlegel, J. Chem. Phys. 90 (1989) 2154;
(c) C. Gonzalez, H.B. Schlegel, J. Phys. Chem. 94 (1990) 5523.
[28] (a) A. Corma, C. del Pino, M. Iglesias, F. Sánchez, J. Chem. Soc. Chem. Commun. (1991) 1253;
(b) A. Corma, M. Iglesias, M.V. Martín, J. Rubio, F. Sánchez, Tetrahedron: Asymmetry 3 (1992) 845;
(c) A. Corma, M. Fuerte, M. Iglesias, F. Sánchez, J. Mol. Catal. A Chem. 107 (1996) 225, and references therein;
(d) M.J. Alcón, A. Corma, M. Iglesias, F. Sánchez, J. Mol. Catal. A Chem. 194 (2003) 137.
[29] P. Pelagatti, in: J.G. de Vries, C.J. Elsevier (Eds.), Handbook of Homogeneous Hydrogenation, vol. 1, Weinheim, Wiley–VCH, 2007, p. 71.
[30] (a) G. Henrici-Olivé, S. Olivé, Angew. Chem. Int. Ed. 13 (1974) 549;
(b) G. Henrici-Olivé, S. Olivé, J. Mol. Catal. 1 (1975/6) 121.
[31] D.R. Armstrong, O. Novaro, M.E. Ruiz-Vizcaya, R. Linarte, J. Catal. 48 (1977) 8.
[32] S. Niu, M.B. Hall, Chem. Rev. 100 (2000) 353.
[33] (a) F. Hutschka, A. Dedieu, W. Leitner, Angew. Chem. Int. Ed. 34 (1995) 1742;
(b) F. Hutschka, A. Dedieu, M. Eichberger, R. Fornika, W. Leitner, J. Am. Chem. Soc. 119 (1997) 4432;
(c) A. Milet, A. Dedieu, G. Kapteijn, G. van Koten, Inorg. Chem. 36 (1997) 3223;
(d) A. Dedieu, S. Humbel, J.E. Cornelis, C. Grauffel, Theor. Chem. Acc. 112 (2004) 305.
[34] D.G. Musaev, R.D.J. Froese, K. Morokuma, S. Strömberg, K. Zetterberg, P.E.M. Siegbahn, Organometallics 16 (1997) 1933.
[35] D.G. Musaev, R.D.J. Froese, K. Morokuma, Organometallics 17 (1998) 1850.
[36] D. Sellmann, F. Geipel, M. Moll, Angew. Chem. Int. Ed. 39 (2000) 561.
[37] Y. Musashi, S. Sakaki, J. Am. Chem. Soc. 122 (2000) 3867.
[38] G. Zampella, M. Bruschi, P. Fantucci, L. De Gioia, J. Am. Chem. Soc. 127 (2005) 13180, and references therein.
[39] (a) F. Hutschka, A. Dedieu, J. Chem. Soc. Dalton Trans. 11 (1997) 1899;
(b) M. Ito, M. Hirakawa, K. Murata, T. Ikariya, Organometallics 20 (2001) 379;
(c) C.A. Sandoval, T. Ohkuma, K. Muñiz, R. Noyori, J. Am. Chem. Soc. 125 (2003) 13490;
(d) V. Rautenstrauch, X. Hoang-Cong, R. Churlaud, K. Abdur-Rashid, R.H. Morris, Chem. Eur. J. 9 (2003) 4954;
(e) C.P. Casey, J.B. Johnson, S.W. Singer, Q. Cui, J. Am. Chem. Soc. 127 (2005) 3100;
(f) C. Hedberg, K. Källström, P.I. Arvidsson, P. Brandt, P.G. Andersson, J. Am. Chem. Soc. 127 (2005) 15083.
[40] V.V. Grushin, Chem. Rev. 96 (1996) 2011.
[41] J. López-Serrano, S.B. Duckett, A. Lledós, J. Am. Chem. Soc. 128 (2006) 9596.
[42] Values used in the Gaussian 03 program package.
[43] (a) R.H. Crabtree, P.E.M. Siegbahn, O. Eisenstein, A.L. Rheingold, T.F. Koetzle, Acc. Chem. Res. 29 (1996) 348;

(b) M.J. Calhorda, Chem. Commun. (2000) 801;
(c) J.G. Planas, C. Viñas, F. Teixidor, A. Comas-Vives, G. Ujaque, A. Lledós, M.E. Light, M.B. Hursthouse, J. Am. Chem. Soc. 127 (2005) 15976.
[44] J.H. Groen, A.D. Zwart, M.J.M. Vlaar, J.M. Ernsting, P.W.N.W. van Leeuwen, K. Vrieze, H. Kooijman, W.J.J. Smeets, A.L. Spek, P.H.M. Budzelaar, Q. Xiang, R.P. Thummel, Eur. J. Inorg. Chem. 00 (1998) 1129.
[45] P. Pelagatti, A. Venturini, A. Leporati, M. Carcelli, M. Costa, A. Bacchi, G. Pelizzi, C.J. Pelizzi, Chem. Soc. Dalton Trans. 16 (1998) 2715.
[46] P.E.M. Siegbahn, J. Am. Chem. Soc. 115 (1993) 5803.
[47] (a) N. Koga, S. Obara, K. Kitaura, K. Morokuma, J. Am. Chem. Soc. 107 (1985) 7109;
(b) D.G. Musaev, M. Svensson, K. Morokuma, S. Strömberg, K. Zetterberg, P.E.M. Siegbahn, Organometallics 16 (1997) 1933;
(c) D.G. Musaev, R.D.J. Froese, M. Svensson, K. Morokuma, J. Am. Chem. Soc. 11 (1997) 367.
[48] D.L. Thorn, R. Hoffmann, J. Am. Chem. Soc. 100 (1978) 2079.
[49] I. Demachy, M.A. Esteruelas, Y. Jean, A. Lledós, F. Maseras, L.A. Oro, C. Valero, F. Volatron, J. Am. Chem. Soc. 118 (1996) 8388.